

# Intramolecular Charge-Transfer Interaction of Donor–Acceptor–Donor Arrays Based on Anthracene Bisimide

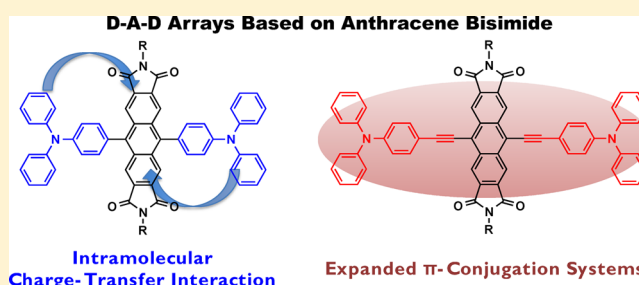
Tetsuo Iwanaga,<sup>\*,†</sup> Marina Ogawa,<sup>†</sup> Tomokazu Yamauchi,<sup>†</sup> and Shinji Toyota<sup>\*,‡</sup>

<sup>†</sup>Department of Chemistry, Faculty of Science, Okayama University of Science, 1-1 Ridaicho, Kita-ku, Okayama 700-0005, Japan

<sup>‡</sup>Department of Chemistry and Materials Science, Tokyo Institute of Technology, 2-12-1 Ookayama, Meguro-ku, Tokyo 152-8551, Japan

**S** Supporting Information

**ABSTRACT:** We designed anthracene bisimide (ABI) derivatives having two triphenylamine (TPA) groups as donor units at the 9,10-positions to form a novel  $\pi$ -conjugated donor–acceptor system. These compounds and their analogues with ethynylene linkers were synthesized by Suzuki–Miyaura and Sonogashira coupling reactions, respectively. In UV–vis spectra, the linker-free derivatives showed broad absorption bands arising from intramolecular charge-transfer interactions. Introducing ethynylene linkers resulted in a considerable red shift of the absorption bands. In fluorescence spectra, the ethynylene derivatives showed intense emission bands at 600–650 nm. Their photophysical and electrochemical properties were compared with those of the corresponding mono TPA derivatives on the basis of theoretical calculations and cyclic voltammetry to evaluate the intramolecular electronic interactions between the donor and acceptor units.



## INTRODUCTION

Aromatic bisimides such as perylene bisimide (PBI) and naphthalene bisimide have been extensively used in the development of new organic materials<sup>1,2</sup> for applications such as organic light-emitting diodes,<sup>3</sup> organic field-effect transistors (OFETs),<sup>4</sup> and organic photovoltaics.<sup>5,6</sup> Recently, Chen and co-workers reported a new type of aromatic bisimide in the construction of a helical structure.<sup>7</sup> Acene-type bisimides such as anthracene-2,3:6,7-bisimides (ABIs)<sup>8</sup> and pentacene-2,3:9,10-bisimide<sup>9</sup> are also promising candidates for constructing various types of functional molecules. For example, the ABI derivatives with 1,5-diphenyl and 9,10-dicyano groups have been used in chemical sensors<sup>8b</sup> and OFETs,<sup>8c,d</sup> respectively. Notably, the fluorescence properties of ABI derivatives are strongly influenced by substitution with arylethynyl groups.<sup>10</sup> Recently, we reported that a donor–acceptor (D–A) array consisting of an aromatic bisimide core and a (9-anthryl)ethynyl group showed interesting spectroscopic properties due to intramolecular charge-transfer (CT) interactions.<sup>11</sup> In a previous report by Shoaee et al., a donor–acceptor–donor (D–A–D) array of PBI derivatives, linked by triphenylamine (TPA) units, showed interesting photophysical properties such as intramolecular photoinduced charge separation in solid films.<sup>12</sup> However, the construction of a D–A–D array of ABI derivatives has not been reported. Therefore, we designed a new D–A–D array of ABI derivatives with TPA donor units linked directly or via ethynylene linkers at the 9,10-positions. Herein we report the photophysical and redox properties of disubstituted ABI derivatives **D2** and **A2** with the aid of DFT calculations. These

results are compared with those of their monosubstituted analogues **D1** and **A1** (Figure 1).

## RESULTS AND DISCUSSION

**Synthesis.** The target ABI derivatives **D2** and **A2** were synthesized from 9,10-dibromo-ABI **1**<sup>8c,d</sup> by cross-coupling reactions (Scheme 1). The Suzuki–Miyaura coupling of **1** with 4-(diphenylamino)benzeneboronic acid pinacol ester **3**<sup>13</sup> under conventional conditions gave **D2** in 77% yield as a reddish brown solid. The Sonogashira coupling of **1** with 4-ethynyltriphenylamine **4**<sup>14</sup> under conventional conditions gave **A2** in 75% yield as a purple solid. Compounds **D1** and **A1** were similarly synthesized from 9-bromo-ABI **2**. These compounds were characterized by NMR and mass spectrometric analyses.

**Molecular Structures.** Because X-ray analyses of the compounds were unsuccessful, the molecular structures of the ABI derivatives were calculated using DFT (Figures S2 and S3, Supporting Information).<sup>15</sup> The structures of *N*-Me derivatives (**D2'**, **A2'**, **D1'**, and **A1'**) as models were optimized at the B3LYP/6-31G(d) theory level. In **D2'**, the two phenyl groups at 9,10-positions are approximately perpendicular to the anthracene plane [with a dihedral angle C(9a)–C(9)–C(4')–C(3') of 84°] to avoid steric interactions. Conversely, the phenyl groups connected to the alkyne carbons in **A2'** are nearly coplanar with the anthracene plane [with a dihedral angle C(9a)–C(9)–C(4')–C(3') of 0.3°] to maximize resonance

Received: February 19, 2016

Published: April 28, 2016

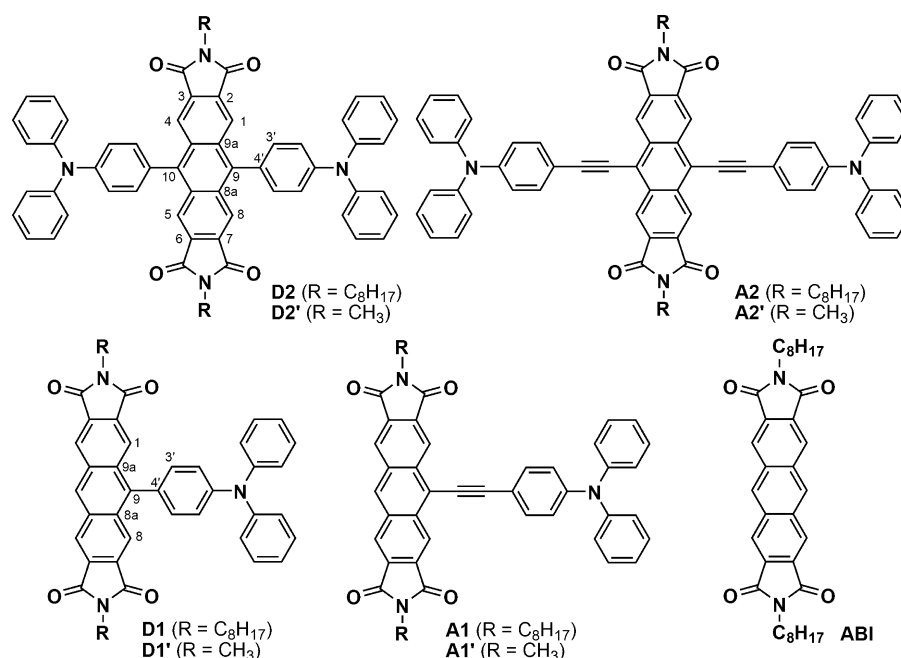
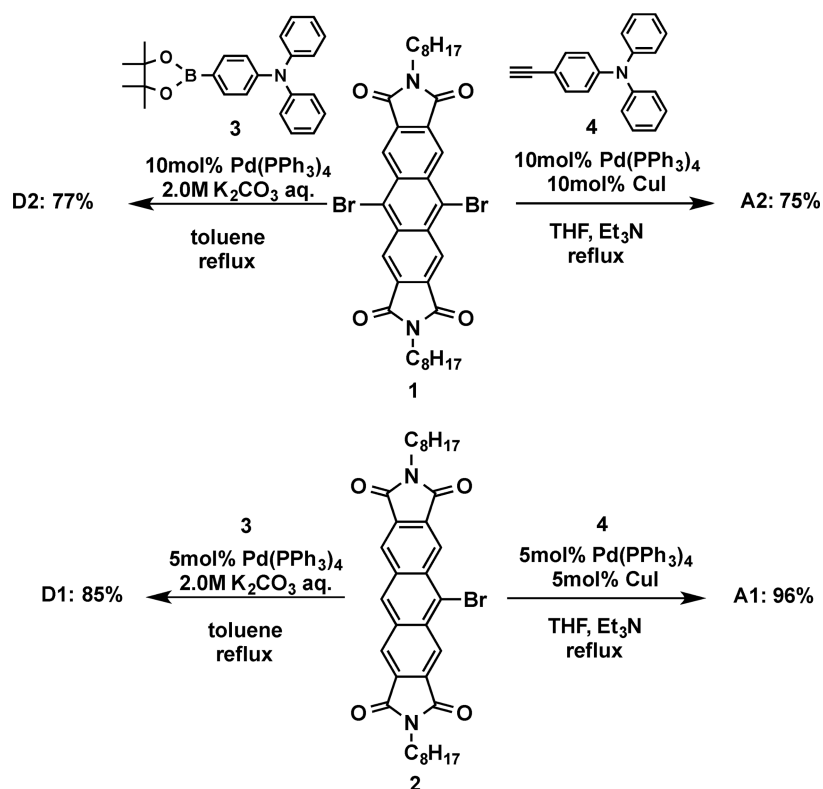


Figure 1. Molecular structures of ABI derivatives with TPA units.

Scheme 1. Synthesis of ABI Derivatives D2, A2, D1, and A1



stabilization.<sup>16</sup> In D1' and A1', the corresponding phenyl groups have similar conformational features.

**Electronic Spectra.** UV-vis and fluorescence spectra of D2, A2, D1, and A1 were measured in CHCl<sub>3</sub> (Figure 2). The spectroscopic data are summarized in Table 1. These compounds showed characteristic broad absorption bands with considerable bathochromic effects in the long-wavelength region, whereas ABI showed structured bands at  $\lambda_{\text{max}} = 421$  nm. For D2 and D1, the shoulder bands red-shifted in this order and

those of D2 extended to 530 nm. The presence of ethynylene linkers considerably enhanced both the bathochromic and hyperchromic effects. In particular, A2 exhibited a broad and intense band at 582 nm, and its peak edge red-shifted by more than 100 nm compared with that of D2. A broad absorption band in A2 is attributed to extension of  $\pi$ -conjugation over the entire molecule. Time-dependent DFT calculations suggested that these bands could be assigned as HOMO to LUMO transitions (Figure 3). The calculated band gap of A2' (2.10 eV)

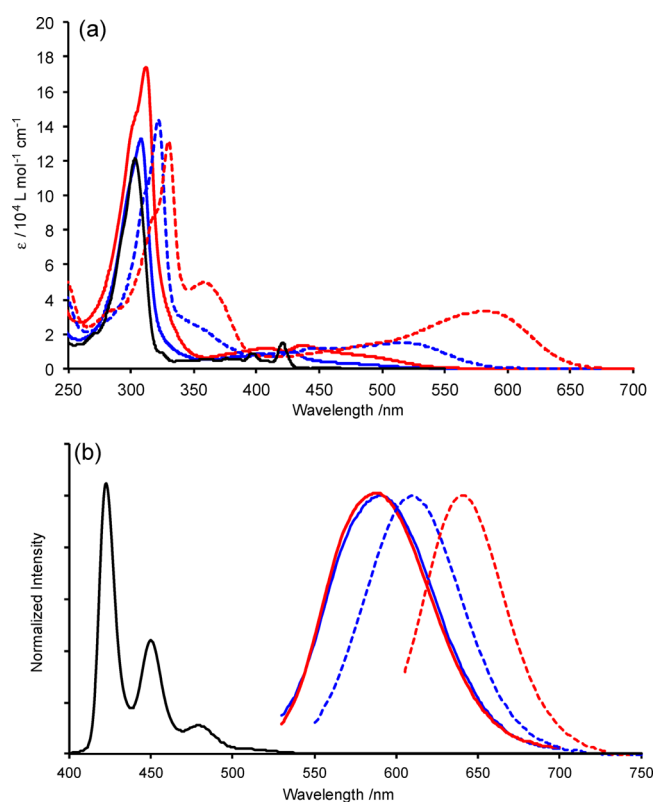


**Figure 2.** (a) UV-vis and (b) fluorescence spectra of ABI derivatives and reference compound ABI in  $\text{CHCl}_3$ . **D2** (solid red), **D1** (solid blue), **A2** (dashed red), **A1** (dashed blue), and **ABI** (solid black).

**Table 1. UV-vis Absorption and Fluorescence Data for the ABI Derivatives and the Reference Compound ABI**

compounds	$\lambda_{\text{max}}$ (nm) ( $\epsilon$ )	calcd $\lambda_{\text{max}}$ ( $f$ ) <sup>b</sup> (nm)	$\lambda_{\text{em}}$ (nm) ( $\Phi_{\text{F}}$ ) <sup>c</sup>	$\tau_{\text{F}}$ (ns) <sup>d</sup>
<b>D2</b>	479 (2800) <sup>a</sup>	573 (0.02)	587 (0.03)	— <sup>e</sup>
<b>D1</b>	427 (11100) <sup>a</sup>	404 (0.09)	591 (0.04)	— <sup>e</sup>
<b>A2</b>	582 (33000)	667 (1.15)	641 (0.53)	3.4
<b>A1</b>	515 (14800)	591 (0.44)	611 (0.39)	4.2
<b>ABI</b>	421 (15000)	397 (0.03)	423 (0.31)	4.2

<sup>a</sup>A shoulder band. <sup>b</sup>Calculated at TD/B3LYP/6-31G(d)//B3LYP/6-31G(d) theory level for the *N*-Me compounds. Only energies with oscillator strength  $f > 0.01$  are shown. <sup>c</sup>Absolute quantum yields determined by a calibrated integrating sphere system in chloroform. <sup>d</sup>Fluorescence lifetimes. <sup>e</sup>Not measured due to weak fluorescence.

was the lowest among the model compounds (Table 2). The calculated MOs of **D2'** indicated that the HOMO and LUMO levels were mainly located on the TPA and the ABI units, respectively (Figure 3). Therefore, the broad absorption peaks of **D2** in the longest wavelength region are attributed to an intramolecular CT interaction.

In their fluorescence spectra, compounds **A2** and **A1** showed strong emission bands at 611 and 641 nm, respectively. An increasing number of TPA-ethynyl groups induces the red shift of emission due to the expanded  $\pi$ -conjugation system. In contrast, compounds **D2** and **D1** showed weak emission bands around 590 nm. Almost the same emission for **D2** and **D1** demonstrated little substitution effect due to the twisted structure between the ABI unit and TPA units. These data show that the ethynylene linkers contributed to the bathochromic effects observed in the absorption spectra. It is worth noting that

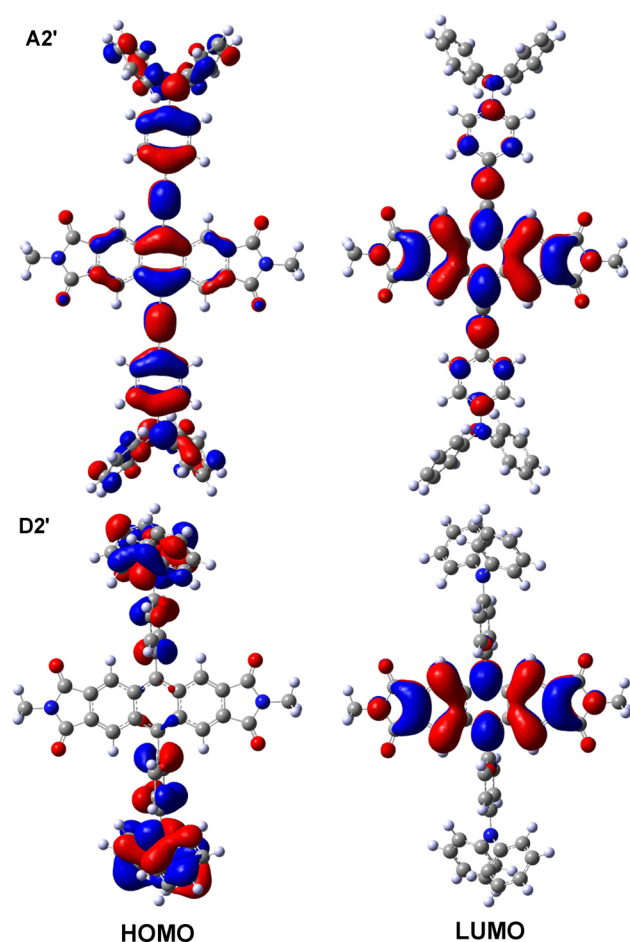


**Figure 3.** MO plots of **A2'** and **D2'** structures calculated at the B3LYP/6-31G(d) theory level.

**Table 2. Electrochemical Data and HOMO–LUMO Energy Gaps of ABI Derivatives**

compounds	$E_{1/2}^{\text{red}}$ (V) <sup>a</sup>	$E_{\text{HOMO}}$ (eV) <sup>d</sup>	$E_{\text{LUMO}}$ (eV) <sup>d</sup>	$E_{\text{g}}$ (eV)	$E_{\text{opt}}$ (eV) <sup>e</sup>
<b>D2</b>	−1.71, −2.02 (−1.74, −2.04) <sup>b</sup>	−5.15	−2.56	2.59	2.59
<b>D1</b>	−1.71, −2.00 (−1.74, −2.06) <sup>b</sup>	−5.21	−2.68	2.53	2.90
<b>A2</b>	−1.44, −1.86 <sup>c</sup>	−4.90	−2.80	2.10	2.13
<b>A1</b>	−1.56, −1.96 <sup>c</sup>	−5.16	−2.79	2.37	2.41
<b>ABI</b>	−1.70, −2.00	−6.29	−2.82	3.47	2.95

<sup>a</sup>Measured in  $\text{CH}_2\text{Cl}_2$  (0.30–1.00 mmol  $\text{L}^{-1}$ ) with *n*- $\text{Bu}_4\text{NClO}_4$  (0.10 mol  $\text{L}^{-1}$ ) as the supporting electrolyte and  $\text{Ag}/\text{Ag}^+$  as the reference electrode. <sup>b</sup>The values of the first and second reduction potentials. <sup>c</sup>Only the reduction potentials due to irreversible waves are shown. <sup>d</sup>Calculated at the B3LYP/6-31G(d) theory level for the *N*-Me derivatives. <sup>e</sup>The optical band gap determined from band onset with a molar absorptivity of  $\epsilon = 500 \text{ L mol}^{-1} \text{ cm}^{-1}$ .

the emission of **A2** and **A1** is dependent on the solvent. A small but significant red shift of **A1** (**A2**) was observed from 580 (627) nm in benzene to 611 (641) nm in  $\text{CHCl}_3$  and 618 (641) nm in THF. These results support that the polarized excited state of **A1** and **A2** is stabilized by the solvent polarity. The fluorescence quantum yields  $\Phi_{\text{F}}$  of **A2** (0.53) and **A1** (0.39) were larger than that of **ABI** (0.31), and their fluorescence life times were comparable to that of **ABI**. The quenching of **D1** and **D2** is attributable to efficient photoinduced electron transfer

from the TPA donor groups to the ABI acceptor unit.<sup>12</sup> The HOMO to LUMO transition is symmetrically forbidden due to the lack of orbital overlap and the perpendicularly arranged aromatic rings.<sup>17</sup> The TPA groups that are directly connected to the ABI unit play a role in the quenching process.<sup>11</sup>

**Cyclic Voltammograms.** Cyclic voltammetry was measured to evaluate the redox properties of the ABI derivatives in CH<sub>2</sub>Cl<sub>2</sub> with *n*-Bu<sub>4</sub>NClO<sub>4</sub> (0.1 M) as the supporting electrolyte (Figure S4, Supporting Information). The observed reduction potentials are listed in Table 2. The TPA groups have almost no influence on the electron-donating ability because ABI unit has weak electron acceptor ability, and thus all compounds are oxidized at +0.61 (D2), +0.60 (D1), +0.57 (A2), and +0.59 (A1) V (Figure S4). Cyclic voltammograms of D1 and D2 consisted of two reversible redox waves at −1.71, −2.00 and −1.71, −2.02 V, as observed for ABI, due to the formation of radical anion and dianion species, respectively. No further anodic shifts were observed from the TPA groups connected to the ABI unit because of poor  $\pi$ -conjugation. A1 exhibited an anodic shift of its  $E_1^{\text{red}}$  and  $E_2^{\text{red}}$  values by 0.15 and 0.04 V compared with D1, because insertion of the  $\pi$ -spacer lowered the LUMO energy level. The presence of two TPA-ethynyl units anodically shifted the reduction potentials of A2 by 0.12 and 0.10 V, respectively, compared with those of A1. This is readily explained by the extended  $\pi$ -conjugation arising from the strong electron-donating ability of two TPA-ethynyl units.

## CONCLUSION

We synthesized a novel D–A–D array of ABI derivatives having two TPA groups at 9,10-positions via Suzuki–Miyaura and Sonogashira coupling reactions. In the absorption spectra, D2, which is directly connected to two TPA groups, demonstrated intramolecular CT bands. A2 exhibited absorption bands at long wavelengths and strong emission bands, attributed to the presence of the ethynylene linker, which extended the  $\pi$ -conjugation. In cyclic voltammetry, A2 and A1 showed irreversible reduction peaks, which indicated extended  $\pi$ -conjugation between the ABI unit and TPA groups. Further studies into the synthesis of ABI derivatives with other donor units and their application to organic electronic devices are in progress.

## EXPERIMENTAL SECTION

9-Bromo-*N,N'*-dioctylanthracenebis(dicarboximide) **1**,<sup>11a</sup> 9,10-dibromo-*N,N'*-dioctylanthracenebis(dicarboximide) **2**,<sup>8c</sup> 4-(diphenylamino)benzeneboronic acid pinacol ester **3**,<sup>13</sup> and 4-ethynyltriphenylamine **4**<sup>14</sup> were prepared according to the method described previously.

**9,10-Bis[4-(diphenylamino)phenyl]-*N,N'*-di-*n*-octylanthracenebis(dicarboximide) (D2).** A solution of 9,10-dibromo-ABI **1** (50.3 mg, 0.072 mmol), boronic acid ester **3** (80.0 mg, 0.22 mmol), and Pd(PPh<sub>3</sub>)<sub>4</sub> (8.55 mg, 7.40  $\mu$ mol, 10 mol %) in a mixture of degassed toluene (7 mL) and 2 M aq K<sub>2</sub>CO<sub>3</sub> (7 mL) was refluxed for 15 h under Ar. The solvent was removed by evaporation. The organic materials were extracted with CH<sub>2</sub>Cl<sub>2</sub> (40 mL). The organic solution was washed with water (40 mL) and brine (40 mL), dried over MgSO<sub>4</sub>, and evaporated. The crude product was purified by chromatography on silica gel with hexane/CHCl<sub>3</sub> (1:1) eluent to give the desired product D2 as a reddish brown solid.

Yield 57.0 mg (77%); mp 286–288 °C. <sup>1</sup>H NMR (CDCl<sub>3</sub>, 400 MHz):  $\delta$  0.86 (t, 6H, *J* = 6.8 Hz), 1.25–1.33 (m, 20H), 1.66–1.71 (m, 4H), 3.75 (t, 4H, *J* = 7.2 Hz), 7.21–7.26 (m, 12H), 7.35–7.42 (m, 16H), 8.40 (s, 4H). <sup>13</sup>C NMR (CDCl<sub>3</sub>, 100 MHz):  $\delta$  14.1, 22.6, 26.9, 28.4, 29.1, 29.2, 31.8, 38.5, 121.4, 124.0, 125.1, 125.8, 127.6, 128.5, 129.6, 131.6, 133.1, 144.2, 147.2, 148.6, 167.7. IR (KBr)  $\nu$  2922, 2854,

1764, 1716, 1589, 1490 cm<sup>−1</sup>; HRMS–FAB: *m/z* [M]<sup>+</sup> calcd for C<sub>70</sub>H<sub>66</sub>N<sub>4</sub>O<sub>4</sub>: 1026.5084; found: 1026.5056.

**9-[4-(Diphenylamino)phenyl]-*N,N'*-di-*n*-octylanthracenebis(dicarboximide) (D1).** This compound was prepared from 9-bromo-ABI **2** (21.1 mg, 0.034 mmol), boronic acid ester **3** (18.1 mg, 0.049 mmol), and Pd(PPh<sub>3</sub>)<sub>4</sub> (1.97 mg, 1.71  $\mu$ mol, 5 mol %) according to a procedure similar to that for the synthesis of D2. The reaction mixture was refluxed for 10 h. The crude product was purified by chromatography on silica gel with hexane/CHCl<sub>3</sub> (1:1) eluent to give the desired product D1 as a red solid.

Yield 22.7 mg (85%); mp 249–255 °C (decomp). <sup>1</sup>H NMR (CDCl<sub>3</sub>, 400 MHz):  $\delta$  0.87 (t, 6H, *J* = 7.2 Hz), 1.26–1.34 (m, 20H), 1.71–1.72 (m, 4H), 3.77 (t, 4H, *J* = 7.2 Hz), 7.13–7.24 (m, 6H), 7.34–7.41 (m, 8H), 8.39 (s, 2H), 8.58 (s, 2H), 8.84 (s, 1H). <sup>13</sup>C NMR (CDCl<sub>3</sub>, 100 MHz):  $\delta$  14.1, 22.6, 26.9, 28.5, 29.1, 29.2, 31.8, 38.6, 121.4, 124.0, 125.0, 125.6, 125.8, 128.0, 128.1, 128.2, 129.6, 131.5, 132.5, 133.3, 133.7, 144.9, 147.2, 148.6, 167.4, 167.7. IR (KBr)  $\nu$  2930, 2858, 1764, 1707, 1592, 1491 cm<sup>−1</sup>; HRMS–FAB: *m/z* [M]<sup>+</sup> calcd for C<sub>52</sub>H<sub>53</sub>N<sub>3</sub>O<sub>4</sub>: 783.4036; found: 783.4060.

**9,10-Bis[4-(diphenylamino)phenylethynyl]-*N,N'*-di-*n*-octylanthracenebis(dicarboximide) (A2).** A solution of 9,10-dibromo-ABI **1** (20.0 mg, 0.028 mmol), Pd(PPh<sub>3</sub>)<sub>4</sub> (3.24 mg, 2.8  $\mu$ mol, 10 mol %), and CuI (0.54 mg, 2.8  $\mu$ mol, 10 mol %) in a mixture of THF (4 mL) and Et<sub>3</sub>N (4 mL) was degassed by freeze-drying three times. After 4-ethynyltriphenylamine **4** (30.2 mg, 0.112 mmol) was added, the solution was refluxed for 15 h under Ar. After evaporation of solvent, the crude product was purified by chromatography on silica gel with hexane/CH<sub>2</sub>Cl<sub>2</sub> (1:2) eluent to give the desired product A2 as a purple solid.

Yield 23 mg (75%); mp 280–285 °C (decomp). <sup>1</sup>H NMR (CDCl<sub>3</sub>, 400 MHz):  $\delta$  0.88 (t, 6H, *J* = 7.0 Hz), 1.19–1.43 (m, 20H), 1.75 (quin, 4H, *J* = 6.6 Hz), 3.80 (t, 4H, *J* = 7.4 Hz), 7.10–7.15 (m, 8H), 7.20 (dd, 8H, *J* = 1.2, 8.6 Hz), 7.34 (t, 8H, *J* = 8.8 Hz), 7.64 (dd, 4H, *J* = 1.6, 6.8 Hz), 9.06 (s, 4H). <sup>13</sup>C NMR (CDCl<sub>3</sub>, 100 MHz):  $\delta$  14.1, 22.6, 27.0, 28.5, 29.2, 29.7, 31.8, 38.6, 84.1, 86.3, 106.8, 113.9, 121.5, 124.1, 124.4, 125.5, 128.9, 129.6, 133.2, 134.0, 146.8, 167.2 (one aromatic peak is missing). IR (KBr):  $\nu$  2925, 2855, 2191, 1764, 1711, 1588, 1493 cm<sup>−1</sup>; HRMS–FAB: *m/z* [M]<sup>+</sup> calcd for C<sub>74</sub>H<sub>66</sub>N<sub>4</sub>O<sub>4</sub>: 1074.5084; found: 1074.5112.

**9-[4-(Diphenylamino)phenylethynyl]-*N,N'*-di-*n*-octylanthracenebis(dicarboximide) (A1).** This compound was prepared from **2** (20.0 mg, 0.032 mmol), 4-ethynyltriphenylamine **4** (17.8 mg, 0.066 mmol), Pd(PPh<sub>3</sub>)<sub>4</sub> (1.86 mg, 1.6  $\mu$ mol, 5 mol %), and CuI (0.30 mg, 1.6  $\mu$ mol, 5 mol %) according to a procedure similar to that for the synthesis of A2. The reaction mixture was refluxed for 15 h. The crude product was purified by chromatography on silica gel with hexane/CHCl<sub>3</sub> (1:1) eluent to give the desired product A1 as a red powder.

Yield 25.0 mg (96%); mp 297–300 °C (decomp). <sup>1</sup>H NMR (CDCl<sub>3</sub>, 400 MHz):  $\delta$  0.87 (t, 6H, *J* = 7.0 Hz), 1.20–1.45 (m, 20H), 1.75 (quint, 4H, *J* = 6.6 Hz), 3.80 (t, 4H, *J* = 7.2 Hz), 7.11–7.16 (m, 4H), 7.21 (dd, 4H, *J* = 1.6, 8.8 Hz), 7.34 (t, 4H, *J* = 8.8 Hz), 7.65 (d, 2H, *J* = 8.8 Hz), 8.47 (s, 2H), 8.65 (s, 1H), 9.08 (s, 2H). <sup>13</sup>C NMR (CDCl<sub>3</sub>, 100 MHz):  $\delta$  14.1, 22.6, 27.0, 28.5, 29.2, 31.8, 38.7, 83.4, 105.6, 113.9, 121.7, 124.1, 124.4, 125.4, 125.9, 128.8, 128.9, 129.6, 132.0, 133.1, 133.5, 134.4, 146.8, 149.3, 167.2, 167.3 (one alkyl peak and one alkyne peak are missing). IR (KBr):  $\nu$  2924, 2856, 2188, 1763, 1711, 1589, 1493 cm<sup>−1</sup>; HRMS–FAB: *m/z* [M]<sup>+</sup> calcd for C<sub>54</sub>H<sub>53</sub>N<sub>3</sub>O<sub>4</sub>: 807.4036; found: 807.4019.

## ASSOCIATED CONTENT

### Supporting Information

The Supporting Information is available free of charge on the ACS Publications website at DOI: 10.1021/acs.joc.6b00364.

General experimental methods and <sup>1</sup>H and <sup>13</sup>C NMR spectra of all new compounds, computational results, cyclic voltammograms, photophysical data, and electronic spectra (PDF)



## AUTHOR INFORMATION

### Corresponding Authors

\*E-mail: [iwanaga@chem.ous.ac.jp](mailto:iwanaga@chem.ous.ac.jp). Tel, fax: +81 86 256 9779.

\*E-mail: [stoyota@cms.titech.ac.jp](mailto:stoyota@cms.titech.ac.jp).

### Notes

The authors declare no competing financial interest.

## ACKNOWLEDGMENTS

This work was partly supported by the Wesco Scientific Promotion Foundation and by the MEXT (Ministry of Education, Culture, Sports, Science, and Technology)-Supported Program for the Strategic Research Foundation at Private Universities, 2009–2013.

## REFERENCES

(1) Aromatic bisimide: (a) Jiang, W.; Ye, L.; Li, X.; Xiao, C.; Tan, F.; Zhao, W.; Hou, J.; Wang, Z. *Chem. Commun.* **2014**, *50*, 1024. (b) Li, C.; Wonneberger, H. *Adv. Mater.* **2012**, *24*, 613. (c) Yue, W.; Lv, A.; Gao, J.; Jiang, W.; Hao, L.; Li, C.; Li, Y.; Polander, L. E.; Barlow, S.; Hu, W.; Di Motta, S.; Negri, F.; Marder, S. R.; Wang, Z. *J. Am. Chem. Soc.* **2012**, *134*, 5770. (d) Gsänger, M.; Oh, J. H.; Könemann, M.; Höffken, H. W.; Krause, A.-M.; Bao, Z.; Würthner, F. *Angew. Chem., Int. Ed.* **2010**, *49*, 740. (e) Chopin, S.; Chaignon, F.; Blart, E.; Odobel, F. *J. Mater. Chem.* **2007**, *17*, 4139. (f) Lang, E.; Würthner, F.; Köhler, J. *ChemPhysChem* **2005**, *6*, 935.

(2) Electronic devices: (a) Klauk, H., Ed. *Organic Electronis: Materials, Manufacturing and Applications*; Wiley-VCH: Weinheim, 2006. (b) Müller, T. J. J.; Bunz, U. H. F., Eds. *Functional Organic Materials*; Wiley-VCH: Weinheim, 2007. (c) Haley, M. M.; Tykewinski, R. R., Eds. *Carbon-Rich Compounds: From Molecules to Materials*; Wiley-VCH: Weinheim, 2006.

(3) OLEDs: Müllen, K.; Scherf, U., Eds. *Organic Light Emitting Devices: Synthesis, Properties and Applications*; Wiley-VCH: Weinheim, 2006.

(4) OFETs: (a) Murphy, A. R.; Fréchet, J. M. *Chem. Rev.* **2007**, *107*, 1066. (b) Anthony, J. E. *Angew. Chem., Int. Ed.* **2008**, *47*, 452. (c) Schmidt, R.; Oh, J. H.; Sun, Y. S.; Deppisch, M.; Krause, A. M.; Radacki, K.; Braunschweig, H.; Könemann, M.; Erk, P.; Bao, Z. A.; Würthner, F. *J. Am. Chem. Soc.* **2009**, *131*, 6215. (d) Wang, H.-Y.; Liu, F.; Xie, L.-H.; Tang, C.; Peng, B.; Huang, W.; Wei, W. *J. Phys. Chem. C* **2011**, *115*, 6961. (e) Yao, L.; Xue, S.; Wang, Q.; Dong, W.; Yang, W.; Wu, H.; Zhang, M.; Yang, B.; Ma, Y. *Chem. - Eur. J.* **2012**, *18*, 2707.

(5) POVs: (a) Brabec, C.; Cyakonov, V.; Scherf, U., Eds. *Organic Photovoltaics*; Wiley-VCH: Weinheim, 2008. (b) Zhang, X.; Lu, Z.; Ye, L.; Zhan, C.; Hou, J.; Zhang, S.; Jiang, B.; Zhao, Y.; Huang, J.; Zhang, S.; Liu, Y.; Shi, Q.; Liu, Y.; Yao, J. *Adv. Mater.* **2013**, *25*, 5791. (c) Wu, Y.; Zhu, W. *Chem. Soc. Rev.* **2013**, *42*, 2039. (d) Zhan, X. W.; Facchetti, A.; Barlow, S.; Marks, T. J.; Ratner, M. A.; Wasielewski, M. R.; Marder, S. R. *Adv. Mater.* **2011**, *23*, 268. (e) Li, C.; Wonneberger, H. *Adv. Mater.* **2012**, *24*, 613. (f) Thompson, B. C.; Fréchet, J. M. *Angew. Chem., Int. Ed.* **2008**, *47*, 58.

(6) (a) Grätzel, M. *Acc. Chem. Res.* **2009**, *42*, 1788. (b) Imahori, H. *J. Mater. Chem.* **2007**, *17*, 31.

(7) (a) Li, M.; Yao, W.; Chen, J.-D.; Lu, H.-Y.; Zhao, Y. S.; Chen, C.-F. *J. Mater. Chem. C* **2014**, *2*, 8373. (b) Li, M.; Niu, Y.; Zhu, X.; Peng, Q.; Lu, H.-Y.; Xia, A.; Chen, C.-F. *Chem. Commun.* **2014**, *50*, 2993.

(8) (a) Morris, J. L.; Becker, C. L.; Fronczek, F. R.; Daly, W. H.; McLaughlin, M. L. *J. Org. Chem.* **1994**, *59*, 6484. (b) Ilhan, F.; Tyson, D. S.; Meador, M. A. *Chem. Mater.* **2004**, *16*, 2978. (c) Wang, Z.; Kim, C.; Facchetti, A.; Marks, T. J. *J. Am. Chem. Soc.* **2007**, *129*, 13362. (d) Usta, H.; Kim, C.; Wang, Z.; Lu, S.; Huang, H.; Facchetti, A.; Marks, T. J. *J. Mater. Chem.* **2012**, *22*, 4459.

(9) (a) Qu, H.; Cui, W.; Li, J.; Shao, J.; Chi, C. *Org. Lett.* **2011**, *13*, 924. (b) Katsuta, S.; Tanaka, K.; Maruya, Y.; Mori, S.; Masuo, S.; Okujima, T.; Uno, H.; Nakayama, K.; Yamada, H. *Chem. Commun.* **2011**, *47*, 10112.

(10) Uejima, M.; Sato, T.; Detani, M.; Wakamiya, A.; Suzuki, F.; Suzuki, H.; Fukushima, T.; Tanaka, K.; Murata, Y.; Adachi, C.; Kaji, H. *Chem. Phys. Lett.* **2014**, *602*, 80.

(11) (a) Iwanaga, T.; Tanaka, R.; Toyota, S. *Chem. Lett.* **2014**, *43*, 105. (b) Iwanaga, T.; Ida, H.; Takezaki, M.; Toyota, S. *Chem. Lett.* **2011**, *40*, 970.

(12) Shoaee, S.; Eng, M. P.; An, Z.; Zhang, X.; Barlow, S.; Marder, S. R.; Durrant, J. R. *Chem. Commun.* **2008**, 4915.

(13) Shi, L.; He, C.; Zhu, D.; He, Q.; Li, Y.; Chen, Y.; Sun, Y.; Fu, Y.; Wen, D.; Cao, H.; Cheng, J. *J. Mater. Chem.* **2012**, *22*, 11629.

(14) Li, Q.; Guo, H.; Ma, L.; Wu, W.; Liu, Y.; Zhao, J. *J. Mater. Chem.* **2012**, *22*, 5319.

(15) Frisch, M. J.; Trucks, G. W.; Schlegel, H. B.; Scuseria, G. E.; Robb, M. A.; Cheeseman, J. R.; Scalmani, G.; Barone, V.; Mennucci, B.; Petersson, G. A.; Nakatsuji, H.; Caricato, M.; Li, X.; Hratchian, H. P.; Izmaylov, A. F.; Bloino, J.; Zheng, G.; Sonnenberg, J. L.; Hada, M.; Ehara, M.; Toyota, K.; Fukuda, R.; Hasegawa, J.; Ishida, M.; Nakajima, T.; Honda, Y.; Kitao, O.; Nakai, H.; Vreven, T.; Montgomery, J. A., Jr.; Peralta, J. E.; Ogliaro, F.; Bearpark, M.; Heyd, J. J.; Brothers, E.; Kudin, K. N.; Staroverov, V. N.; Kobayashi, R.; Normand, J.; Raghavachari, K.; Rendell, A.; Burant, J. C.; Iyengar, S. S.; Tomasi, J.; Cossi, M.; Rega, N.; Millam, J. M.; Klene, M.; Knox, J. E.; Cross, J. B.; Bakken, V.; Adamo, C.; Jaramillo, J.; Gomperts, R.; Stratmann, R. E.; Yazyev, O.; Austin, A. J.; Cammi, R.; Pomelli, C.; Ochterski, J. W.; Martin, R. L.; Morokuma, K.; Zakrzewski, V. G.; Voth, G. A.; Salvador, P.; Dannenberg, J. J.; Dapprich, S.; Daniels, A. D.; Farkas, Ö.; Foresman, J. B.; Ortiz, J. V.; Cioslowski, J.; Fox, D. J. *Gaussian 09, Revision C.01*, Gaussian, Inc., Wallingford, CT, 2009.

(16) Toyota, S. *Chem. Rev.* **2010**, *110*, 5398.

(17) (a) Grabowski, Z. R.; Rotkiewicz, K.; Rettig, W. *Chem. Rev.* **2003**, *103*, 3899. (b) Rotkiewicz, K.; Grellmann, K. H.; Grabowski, Z. R. *Chem. Phys. Lett.* **1973**, *19*, 315.

## NOTE ADDED AFTER ASAP PUBLICATION

Figure 1 contained errors in the version published ASAP April 28, 2016; the correct version reposted on May 2, 2016.